IEEE Robotics and Automation Letters (RAL) paper presented at the
2020 IEEE/RSJ International Conference on Intelligent Robots and Systems (IROS)
October 25-29, 2020, Las Vegas, NV, USA (Virtual)

MILiMAC: Flexible Catheter with Miniaturized Electromagnets as a Small-Footprint System for Microrobotic Tasks

Jakub Sikorski, Sumit Mohanty and Sarthak Misra

***Abstract*— Advancements in medical microrobotics have given rise to an abundance of agents capable of localised interaction with human body in small scales. Nevertheless, clinically-relevant applications of this technology are still limited by the auxiliary infrastructure required for actuation of micro-agents. In this paper, we approach this challenge. Using finite-element analysis, we show that miniaturization of electromagnets can be used to create systems capable of providing magnetic forces adequate for micro-agent steering, while retaining small footprint and power consumption. We use these observations to create MILiMAC (Microrobotic Infrastructure Loaded into Magnetically-Actuated Catheter). MILiMAC is a flexible catheter employing three miniaturized electromagnets to provide localized magnetic actuation at the deeply-seated microsurgery site. We test our approach in a proof-of-concept study deploying MILiMAC inside a test platform to deliver and steer a 600 [μm] ferromagnetic microbead. The bead is steered along a set of user-defined trajectories using closed-loop position control. Across all trajectories the best performance metrics are the mean error of 0.41 [mm] and the steady-state error of 0.27 [mm].**

I. Introduction

Microrobotic surgery is a future medical technology with the potential of revolutionising the way clinicians interact with human body. Employing functional miniaturized agents and controlling them *in vivo* could allow for localized and selective engagement of human body on cellular and tissue organization levels [1]. Such capabilities would complement contemporary medicine, which excels in procedures targeting entire organs, as well as in systemic treatment through delivery of therapeutic substances via the bloodstream.

The potential of microrobotic surgery has been so far predominantly demonstrated in an abundance of *in vitro* experiments performed with miniaturized milli- and micro-agents. These agents are often designed with a specific surgical tasks in mind and fabricated using sophisticated techniques [2]. Prominent examples involve: soft grippers for single-cell biopsy [3], scaffold-type robots for stem cell manipulation [4], thermoactive polymers for targeted drug delivery [5], stress-engineered MEMS microrobots [6], tubular micromotors, such as spermbots or microjets [7], and helical microswimmers [8]. With recent advancements in soft materials and microfabrication techniques, the surge of new micro-agents is expected to continue [9].

This research has received funding from the European Research Council (ERC) under the European Union's Horizon 2020 Research and Innovation programme (Grant Agreement #638428 - project ROBOTAR).

J. Sikorski, S. Mohanty and S. Misra are with Surgical Robotics Laboratory, Department of Biomechanical Engineering, University of Twente, 7500 AE Enschede, The Netherlands. (j.sikorski@utwente.nl; s.mohanty@utwente.nl; s.misra@utwente.nl)

J. Sikorski and S. Misra are also with the Department of Biomedical Engineering, University of Groningen and University Medical Centre Groningen, 9713 GZ Groningen, The Netherlands.

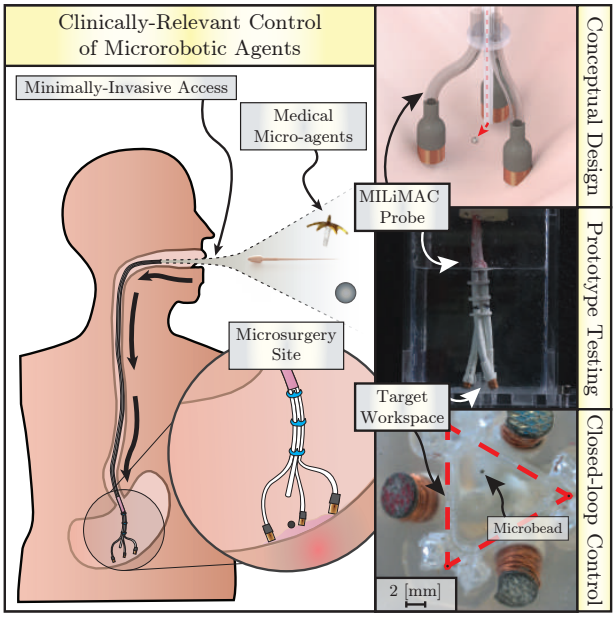

Fig. 1. In this paper, we exploit the concept of electromagnet miniaturization, creating Microrobotic Infrastructure Loaded into Magnetically-Actuated Catheter (MILiMAC). To our best knowledge, MILiMAC is the first device capable of providing localized means of steering magnetic micro-agents from within the human body. For that purpose, MILiMAC is inserted into the body in a minimally-invasive fashion and deployed at the site, where the microsurgery is to be conducted. Subsequently, various micro-agents can be delivered into the target workspace created by the catheter, and steered using miniaturized electromagnets.

Due to their size, a vast majority of these micro-agents cannot rely on internal power sources and sensors for actuation and localization. Hence, they need auxiliary robotic infrastructure to assist them in successful operation [10]. In contrast to the rapid advancements in the design of micro-agents, as described above, the driving concepts behind the auxiliary infrastructure have not changed significantly in the last decade.

Clinically-relevant sensing of micro-agents remains an ongoing challenge, hampering attempts for controlling them *in vivo* [11]. Techniques used to actuate micro-agents, predominantly employing magnetic interaction, are somewhat more mature [12]. Nevertheless, in most cases they still follow the trend initiated by the OctoMag system, using sources of external magnetic field located outside of the body to exert wrenches on magnetic domains within the agents [13]–[15]. Modifications of this approach involve the use of mobile magnetic sources, however, these have been predominantly used for non-contact actuation of mesoscale medical devices [16]–[18].

Despite their prevalence in literature and success with various micro-agents during *in vitro* experiments, magnetic actuation systems located outside of the patient are inherently

burdened with major disadvantages. Large electromagnets are required to generate adequate magnetic fields in deeply seated regions, such as the heart or the stomach [19]. This is particularly problematic when employing static coils, as the workspace of such a system must span a significant portion of human body [20]. Since the task workspace for micro-agents is several orders of magnitude smaller, these systems can be considered overscaled for that purpose. This situation is particularly challenging in presence of internal biological motion, which involves large displacements of tissues around the surgery site due to respiration, peristalsis or blood flow [21].

Furthermore, even the sheer delivery of micro-agents into a desired workspace remains challenging. Current literature usually assumes the micro-agents would be injected into the bloodstream and guided over large distances to the desired, deeply seated location [22]. These distances are several orders of magnitude larger than the micro-agents themselves. Free release of the agents into the body inherently subjects them to a variety of unpredictable biomechanical forces present in complex *in vivo* environments [11]. Due to related challenges, contemporary approaches to delivery and control of micro-agents have yet to provide plausible scenarios of clinically-relevant microsurgical procedures, making room for an alternative.

In this paper, we reconsider the classical infrastructure used for delivery and control of micro-agents. We demonstrate that the forces available for microrobotic control increase as the magnetic actuation system, along with the available workspace are scaled down in size. The implications of that motivate stepping away from using electromagnets located outside the patient. Instead we propose to miniaturize them to the size of a few millimetres. The small footprint of such devices enables their delivery directly into the microsurgery site using tools for minimally-invasive surgery. Magnetic actuation systems integrated on catheters, endoscopes and needles have a potential of bridging the scales of the clinician and the agents and cells, providing well-defined and stable workspace for microsurgeries within the body.

We demonstrate the feasibility of this approach creating a system for steering of micro-agents, which is inspired by endovascular catheters and endoscopes [23]. Microrobotic Infrastructure Loaded into Magnetically-Actuated Catheter (MILiMAC) (Figure 1) is a device with three miniaturized electromagnets, which can be delivered to a deeply seated microsurgery site and deployed, creating a two-dimensional target workspace. Within that workspace, MILiMAC can be used to actuate a wide range of micro-agents.

We test the MILiMAC in an experimental scenario involving delivery and control of a ferromagnetic microbeads. Such microbeads are reliable micro-agents, which can be purposed to carry bioactive substances [24]. The catheter is inserted into a target workspace located at the distal end of a long channel imitating an anatomical duct. The bead is injected into that workspace through MILiMAC and controlled using miniaturized electromagnets along a set of predefined trajectories. Optical tracking is used for closed-loop control. Nevertheless, we also discuss the possibility of using on-site clinically-relevant modalities.

The rest of the paper is structured as follows. Section II introduces the concept of miniaturized electromagnets, presenting its advantages over current approach. Section III presents the design of MILiMAC. Section IV highlights the methods of the proof-of-concept study, including experimental setup. The control algorithm utilizing magnetic forces to move a microbead with MILiMAC is presented in Section V. Section VI contains the results of proof-of-concept validation and the discussion that follows. Finally, the entire paper is summarised by Section VII, proposing next steps to bring our approach closer to clinical practice.

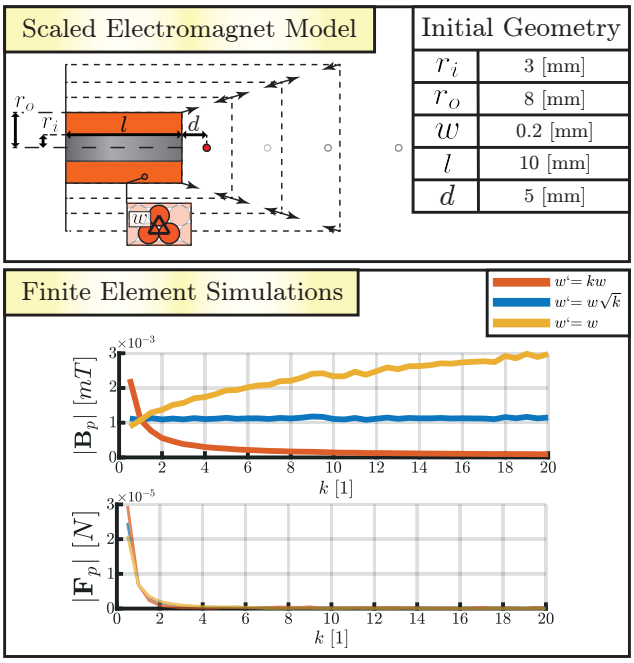

Fig. 2. The results of finite-element (FE) simulations showing the effects of scale on the magnetic field generated by an iron-cored electromagnets. This simulation employs a scalable model following the convention proposed in our previous work [23]. In the model a scalable electromagnet is defined by the radius of the core ($r_i \in \mathbb{R}_+$), outer radius of the coil ($r_0 \in \mathbb{R}_+$), wire diameter ($w \in \mathbb{R}_+$) and length ($l \in \mathbb{R}_+$). We select and a measurement point (marked with red dot) at a distance ($d \in \mathbb{R}_+$), at which we measure the magnitudes of magnetic field ($|\mathbf{B}_p| \in \mathbb{R}_+$) and magnetic force ($|\mathbf{F}_p| \in \mathbb{R}_+$) to be exerted on an iron sphere with a diameter of 1 [mm] located at the measurement point. We use the model to run a series of simulations, where the initial geometry of the model is scaled by a given constant factor ($k = 0.5, 1, 1.5, \ldots, 20$), with three different laws for the scaled wire diameter ($w' \in \mathbb{R}^+$). The distance (d) is scaled by the same factor as the coil to preserve the relative location of the workspace. Our study show that the forces available for magnetic actuation can be significantly increased by miniaturizing the electromagnets.

II. The Effect of Scale on Magnetic Actuation Systems

Magnetic interaction is exploited extensively as a principal method of non-contact actuation of micro-agents. It occurs between any micro-agent with magnetic properties represented by magnetic dipole moment $\left(\mathbf{m}_a \in \mathbf{R}^3\right)$ and the external magnetic field $\left(\mathbf{B}(\mathbf{p}) = \begin{bmatrix} B_x & B_y & B_z \end{bmatrix}^T \in \mathbf{R}^3\right)$ at the location of the agent $\left(\mathbf{p} \in \mathbf{R}^3\right)$. Under the influence of that field, micro-agent experiences a magnetic wrench

$$\mathbf{W} = \begin{bmatrix} \mathbf{F}_\mu \\ \boldsymbol{\tau}_\mu \end{bmatrix} = \begin{bmatrix} \nabla \left(\mathbf{m}_a^T \mathbf{B}(\mathbf{p})\right) \\ \mathbf{m}_a \times \mathbf{B}(\mathbf{p}) \end{bmatrix} \in \mathbb{R}^6. \tag{1}$$

This wrench can be controlled by influencing $\mathbf{B}(\mathbf{p})$ and its spatial gradient using magnetic actuation systems comprising

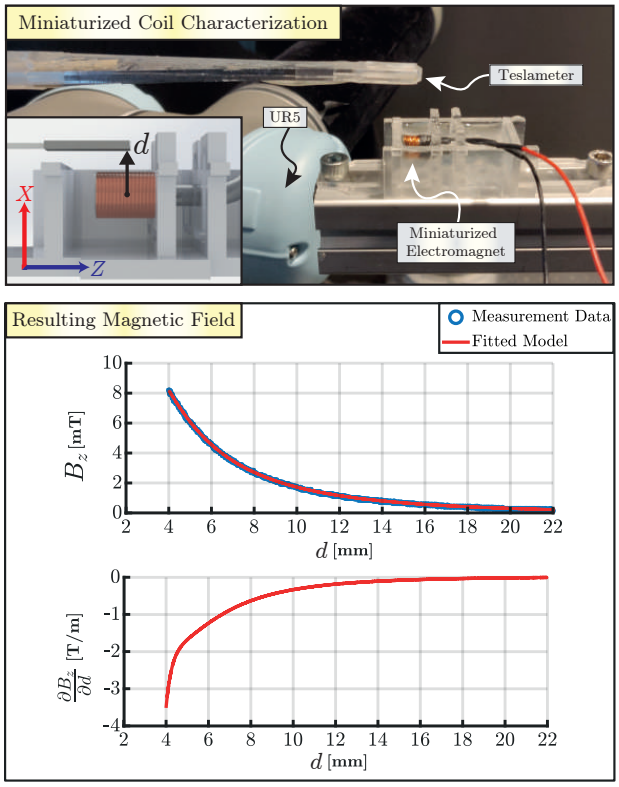

Fig. 3. We characterize a prototype miniaturized electromagnet by measuring the magnetic field $(B_z \in \mathbb{R})$ it generates along the distance $\left(d \in \mathbb{R}^+\right)$ at 1 [A]. The measurements are performed with a Senis 3MH3A-500MT (Senis AG, Baar, Switzerland) teslameter mounted on UR5 robotic arm (Universal Robots, Odense, Denmark). Furthermore, we obtain magnetic field gradient $\left(\frac{\partial B_z}{\partial d} \in \mathbb{R}\right)$ by fitting a rational function over the measured data.

of electromagnets or permanent magnets.

The requirements imposed on magnetic actuation systems are agent-specific, due to diverse methods for using magnetic wrenches to achieve the desired behaviour of a particular agent. Nevertheless, in majority of applications one of the principal design criteria involves making the system capable of generating sufficiently high wrenches $(\mathbf{W})$, thus maximizing magnetic fields/gradients. Conventional way of solving this requirement involves maximizing the power of magnetic field sources. Exploiting the effects of scale on magnetic actuation systems offers an alternative solution.

While considering a simple point-dipole model, the resulting distribution of the magnetic fields remains constant, whereas the gradients decrease by the same factor by which the source is scaled. [13] However, this conjecture does not precisely describe the behaviour of cored electromagnets. As they are complex devices, their magnetic field distribution depends on factors like the number of windings (determined by wire diameter), which do not necessarily scale in a straightforward fashion. Therefore, to represent their behaviour more accurately, we create a scalable FE model (Figure 2) of an iron-core electromagnet acting on a bead located at distance $(\mathbf{d} \in \mathbb{R}^+)$ using the approach presented in our previous work [23]. The distance $(\mathbf{d})$ is scaled by the same factor the geometry of the coil, to show the effect of changing workspace. We estimate magnetic field $(\mathbf{B}(\mathbf{d}))$ under constant current for a range of k. Furthermore, for each simulation we also measure $\left(\nabla \mathbf{B} \in \mathbb{R}^{3\times3}\right)$ indirectly, by estimating the magnitude of the magnetic force $(\mathbf{F}_\mu)$ acting on a constant-size permanent magnet at $\mathbf{d}$.

The simulations performed with our scalable model indicate that, while the magnetic field distribution does depend on a particular scaling method (Figure 2) for wire diameter, the magnitude of the magnetic force $(\mathbf{F}_\mu)$ decreases sharply with k in all simulated cases. As the scale of the model increases from 1 to 20, the forces are reduced in size by three orders of magnitude. This notion indicates that miniaturization of systems for magnetic actuation is a valid way of increasing the magnetic gradients available for steering of micro-agents.

We test this experimentally, by characterizing a prototype miniaturized electromagnet (see Figure 3). Each dimension of the magnet is approximately one order of magnitude smaller than the ones used in conventional systems, which reduces the total volume occupied by it by three orders of magnitude. The results confirm the findings from FE analysis. Rated at a maximum of 2 [A], our miniaturized electromagnet provides gradients of up to 2-3 [T/m] and fields of up to 10-12 [mT], which is comparable with the state-of-the-art systems discussed in [15]. In the same time, the electromagnet has largely minimized footprint and low power consumption of approx. 6 [W]. Using such actuators as building blocks in magnetic actuation systems can reduce the means necessary for microrobotic control.

III. MILiMAC: Flexible Catheter with Miniaturized Electromagnets

Despite the advantages discussed in previous section, magnetic actuation employing miniaturized electromagnets necessitates that the system is deployed at a distance of a few centimetres from the microsurgery site to be effective. This requirement inherently inspires revision of the classical paradigm, whereby the auxiliary magnetic actuation system is located outside of the body of the patient. Utilizing the small footprint of the miniaturized electromagnets, we propose to bring them close to the microsurgery site, a task possible using modern flexible surgical tools. As a consequence, we provide an alternative, minimalist approach to magnetic actuation.

We propose to use a flexible catheter to introduce miniaturized electromagnets into deeply seated body regions in a minimally invasive fashion. The minimum viable design

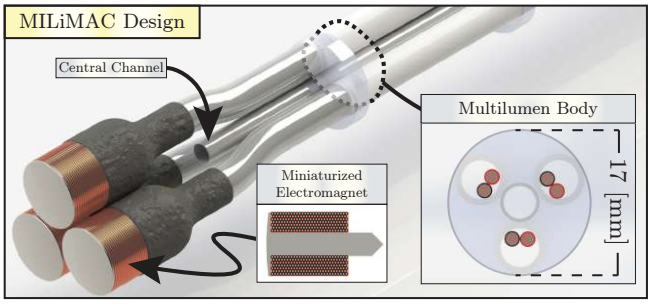

Fig. 4. MILiMAC (Microrobotic Infrastructure Loaded into Magnetically-Actuated Catheter) is a proof-of-concept device, demonstrating the clinical relevance of localized magnetic actuation of micro-agents using miniaturized electromagnets. Three of such electromagnets are distributed radially along a central channel of MILiMAC, which is used for micro-agent delivery. Due to its flexible multilumen body, MILiMAC can be inserted into natural orfices of human body, delivering microrobotic infrastructure to deeply-seated regions.

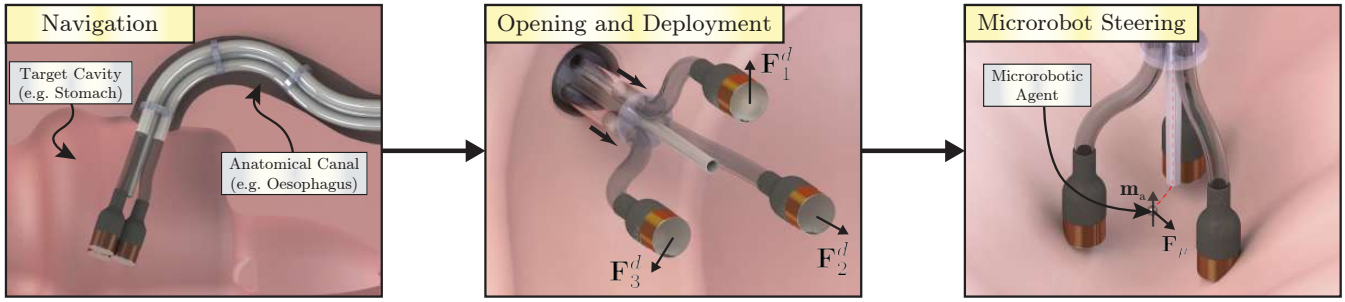

Fig. 5. The proposed mode of operation of MILiMAC (Micorobotic Infrastructure Loaded into Magnetically-Actuated Catheter). The sleek shape and compliant structure of MILiMAC enable navigation to microsurgery sites through natural anatomical canals to deliver miniaturized electromagnets into deeply seated regions, such as stomach. Upon reaching the site, the catheter is deployed by running equal currents through all coils. The resulting repulsive forces $\left(\mathbf{F}_i^d \in \mathbf{R}^3\right)$ open MILiMAC by deflecting the electromagnet tethers away from one another. Open MILiMAC can be pressed against a surface, using friction to lock the coils in place and form target workspace. In this study, we use MILiMAC to steer ferromagnetic microbeads, as these micro-agents display both clinical relevance and properties favourable for magnetic steering. When placed in external magnetic field, a microbead becomes magnetized, with a resulting magnetic dipole moment $\left(\mathbf{m}_a \in \mathbf{R}^3\right)$. Such a magnetized microbead experiences magnetic force $\left(\mathbf{F}_\mu \in \mathbf{R}^3\right)$ dependent on gradients of the field at its location. We control this force by steering currents within MILiMAC coils.

of MILiMAC (Figure 4) employs three electromagnets on flexible tethers fitted at a distal end of a multilumen catheter, which also provides a central channel used for delivery of micro-agents. The sleek shape of MILiMAC allows for insertion into the microsurgery site in a minimally-invasive fashion through the natural orifices of human body (Figure 5) Upon reaching this site, the catheter is opened by running identical currents run through all coils. The resulting repulsive magnetic forces deflect the MILiMAC tethers away from one another. Open catheter is positioned within the microsurgery site, using friction to lock the coils in place. This way, we form a well-defined workspace, into which micro-agents are subsequently delivered through the central channel of MILiMAC.

In contrast to classical, macroscale magnetic actuation systems, symmetry axes of all MILiMAC electromagnets are parallel. During the proof-of-concept validation presented in the next section, we use ferromagnetic microbeads, which can readily be manipulated with parallel electromagnets by exploiting magnetic forces (Figure 4). Despite their simple composition, microbeads can be coated with a wide range of substances to realise tasks such as targeted drug delivery [25].

IV. Proof-of-Concept Validation

Since our catheter is designed to eventually become a clinically-relevant tool, we create an experimental setup to demonstrate the operation of MILiMAC in a procedure emulating the full workflow demonstrated in Figure 4. Albeit not as challenging, as *in vivo* deployment and control, this experiment highlights the advantages of MILiMAC, serving as a foundation for future development towards clinical use.

The prototype of the MILiMAC and the experimental setup for proof-of-concept validation are shown in Figure 6. The catheter comprises of three miniaturized electromagnets with the dimensions as in Section II. The coils are fitted on silicone tethers (length 100 [mm], diameter 4.8 [mm]) located symmetrically around a HDPE (high-density polyethylene) 7.5 [Fr.] endovascular sheath (Maquet, Mahwah, NJ, USA) used as a central channel. The proximal end of the central channel provides a syringe port, used for injection of 600 [μm] 440C stainless steel microbeads (MiSUMi Corporation, Tokyo, Japan) into the target workspace. Each miniaturized electromagnet is powered by a dedicated iPOS4808 BX-CAT servo drive (Technosoft S.A., Neuchâtel, Switzerland). The current used during the microrobot steering is limited to a maximum 2 [A], whereas during the deployment phase a current of 6 [A] is used to deflect the tethers of MILiMAC. The drives are connected to a research laptop through EtherCAT network (control rate 650 [Hz]).

The target workspace has been delimited by a triangular

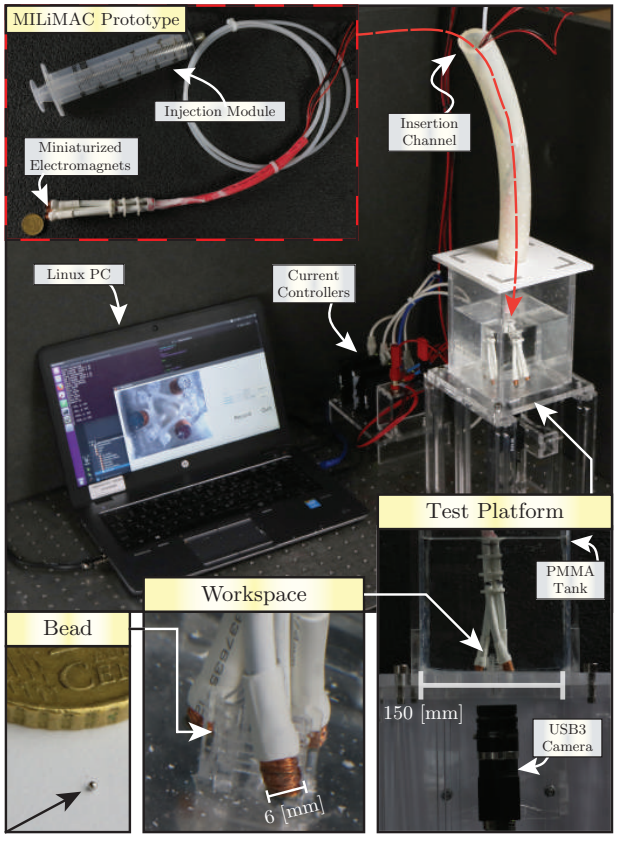

Fig. 6. MILiMAC (Micorobotic Infrastructure Loaded into Magnetically-Actuated Catheter) is validated using a custom test platform, which comprises of a target workspace at the bottom of an acrylic tank. A prototype of MILiMAC is inserted into the tank through a long channel, imitating an anatomical duct. It is deployed around the workspace and monitored by FLIR BlackflyS USB3 Camera (FLIR Systems, Wilsonville, USA). Subsequently, the injection module comprising of a valved syringe at the proximal end of MILiMAC is used to deliver a 600 [μm] microbead into the workspace. Finally, the bead is steered along a set of trajectories, using closed-loop control.

reservoir located at the bottom of a larger acrylic tank filled with water. The catheter is inserted into the tank by an opening in its top wall, accessed through a 40 [cm] long silicone tube imitating an anatomical duct, such as an oesophagus. The operator inserts the MILiMAC through the tube, deploys the tethers as shown in Figure 4. and positions it around triangular reservoir. Once the catheter is in place, a ferromagnetic microbead is injected through the central channel.

FLIR Blackfly S-USB3 camera (FLIR Systems, Wilsonville, OR, USA) is used to image the workspace from below through the transparent floor of the container. The position of the agent is estimated by a segmentation-based tracker similar to our previous work [15]. The resulting information, along with real-time feedback on the location of the microbead are employed to steer it along a set of predefined trajectories. To achieve this, we develop a closed-loop position control algorithm presented in the following section.

V. Position Control using MILiMAC

The key part of the experiment involves autonomous steering of a microbead using coils provided by the MILiMAC. This task is executed on a 2D plane, which we assume to be horizontal. This allows us to neglect the effect of gravity.

Under such conditions, the steering task reduces to tracking a planar trajectory, defined as a set of points $\left(\mathbf{p}_r \in \mathbb{R}^2\right)$. We realise this task by implementing a closed-loop position controller, which utilizes feedback from the optical tracking system. This feedback includes the location of the microbead $\left(\mathbf{p}_a \in \mathbb{R}^2\right)$, and the position $\left(\mathbf{p}_i \in \mathbb{R}^2\right)$ of each coil $(i = 1, 2, 3)$ with respect to the global frame of reference. This frame is shown in Figure 7, which shows the task space as seen by the camera and illustrates the approach we propose.

The total magnetic field at $\mathbf{p}_a$ is the superposition of contributions from all coils. As a result, the bead becomes magnetised and gains magnetic dipole moment $(\mathbf{m}_a)$, with the value proportional to the field up to saturation, which usually happens in the range of 1-2 [T]. Nevertheless, to avoid quadratic dependence of the actuation force on the magnetic field we assume that $\mathbf{m}_a$ is constant and naturally aligned with the magnetic field, which is a common approach taken in the subject. [3]

As gravity prevents off-plane motion of the microbead, it is useful to assume that all magnetic elements taking part in the interaction: the ferromagnetic microbead and the miniaturized electromagnets, are parallel and located on the task plane. The configuration of MILiMAC electromagnets (as shown in Figure 4) restricts the possible values of the magnetic field to

$$\mathbf{B}(\mathbf{p}) = \begin{bmatrix} 0 & 0 & B_z \end{bmatrix}^T. \tag{2}$$

We use this assumption to transform the equation (1). We derive the model relating planar magnetic force $\left(\mathbf{F}_a \in \mathbb{R}^2\right)$ exerted on the microbead by MILiMAC

$$\mathbf{F}_a = \|\mathbf{m}_a\| \begin{bmatrix} \frac{\partial B_z}{\partial x} & \frac{\partial B_z}{\partial y} \end{bmatrix}^T = \|\mathbf{m}_a\| \begin{bmatrix} \boldsymbol{\beta}(\mathbf{p}_1) & \boldsymbol{\beta}(\mathbf{p}_2) & \boldsymbol{\beta}(\mathbf{p}_3) \end{bmatrix} \mathbf{I}, \tag{3}$$

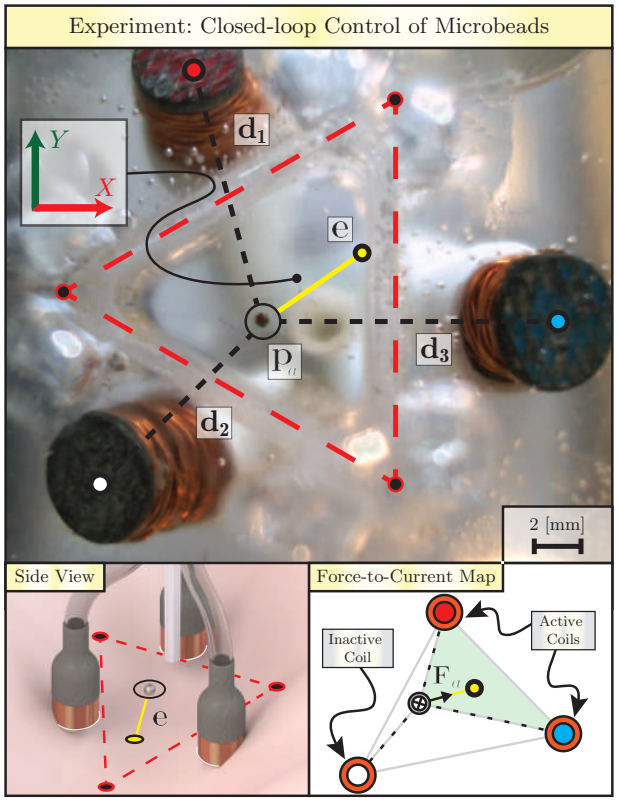

Fig. 7. MILiMAC (Micorobotic Infrastructure Loaded into Magnetically-Actuated Catheter) is used to steer ferromagnetic microbead along point-to-point trajectories (yellow dot) employing closed-loop control. The catheter deployed around a triangular reservoir (red lines). Tracking system is used to provide locations (red, white and blue dots) of MILiMAC coils $(i = 1, 2, 3)$ and the position $\left(\mathbf{p}_a \in \mathbb{R}^2\right)$ of the microbead. This information is used to calculate: the error $\left(\mathbf{e} \in \mathbb{R}^2\right)$ between actual and reference position, and the relative distances $\left(\mathbf{d}_i \in \mathbb{R}^2\right)$ from the microbead to each coil. These distances are required by a force to current map relating the output of a PI controller to the currents in MILiMAC coils. The map employs selective activation of coils to rely on pulling for force generation.

to the currents $\left(\mathbf{I} \in \mathbb{R}^3\right)$ through miniaturized electromagnets. The coil specific model $\left(\boldsymbol{\beta}(\mathbf{p}_i) \in \mathbb{R}^2\right)$ corresponds to the gradients per unit current calculated using the data from coil characterization (Figure 3).

We control the system by using the following modification of the standard PI law:

$$\mathbf{F}_a(\mathbf{e}) = \left(K_p \, \|\mathbf{e}\| + K_i \int_{t_0}^{t} \|\mathbf{e}\| \, dt\right) \widehat{\mathbf{e}}, \tag{4}$$

to calculate the virtual actuation force in the direction of the error $(\mathbf{e} = \mathbf{p}_r - \mathbf{p}_a)$. The magnitude of the actuation force is controlled by the PI action, with performance defined by gains $(K_p, K_i \in \mathbb{R}_+)$. The total value of the integral control is reset whenever $\|\mathbf{e}\|$ falls below 0.1 [mm]. The model (3) can be inverted to map any $\mathbf{F}_a$ to corresponding control currents $(\mathbf{I})$.

Inverting the model (3) using Moore-Penrose pseudoinverse is likely to provide a solution assigning negative current to at least one of the coils. As observed experimentally, this situation leads to unpredictable violations of assumption about constant value and direction of $\mathbf{m}_a$, causing stability problems and requiring alternate control framework, beyond the proof-of-concept scope of this paper. [15] Nevertheless, the operation of MILiMAC with simple PI controller can still be effectively realised by introducing an intermediate step,

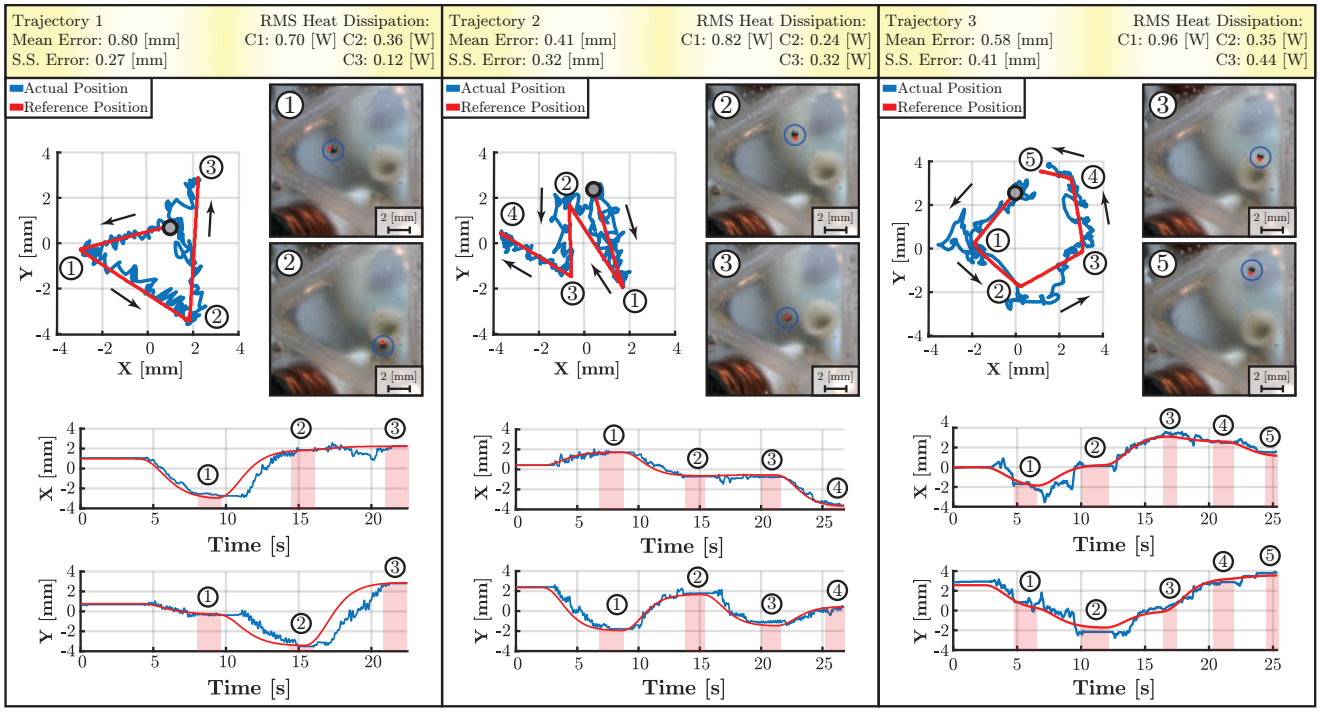

Fig. 8. We test the prototype of the MILiMAC by controlling the microbead along a set of point-to-point trajectories. Three representative trajectories are defined on-the-go by the user, who selects instantaneous target point using user-guided interface. Smooth trajectories between the target points (marked with numbers) are generated using low-pass filter. The top plots show the 2D position plot for each trajectory, whereas the bottom show the time evolution of both coordinates of the position of the microbead. Gray circles on each 2D plot are used to indicate the size of the microbead. For each trajectory the root mean square (RMS) heat dissipation of each coil (C1, C2, C3) and the mean position error is calculated. Since the steady-state (S.S.) error of the system is generally lower than the mean due to the rolling motion, we additionally calculate the error for the S.S. regions, marked with red trapezoids on the time plots. **Please refer to the supporting video material for the demonstration of this experiment.**

in which only two coils of MILiMAC are selected to actuate the bead at any instance of time. These coils are selected based on the direction of the force $\mathbf{F}_a$, such that the magnetic interaction is used solely for pulling (see Figure 7). We use that property in our control scheme to map the actuation force to only the currents $\left(\mathbf{I}_a \in \mathbb{R}^2_+\right)$ for the selected coils $(a_1, a_2 \in i)$ as follows:

$$\mathbf{I}_a = \frac{1}{m_a}\left[\boldsymbol{\beta}(\mathbf{d}_{a_1})\ \boldsymbol{\beta}(\mathbf{d}_{a_2})\right]^{-1}\mathbf{F}_a, \tag{5}$$

whereas keeping third coil unpowered. The resulting currents are always positive, ensuring predictable magnetization of the microbead.

The forces contributing to static friction are a significant factor limiting reliable motion of ferromagnetic beads smaller than 1.2 [mm] in large parts of the workspace. We provide a solution to that problem by revisiting the assumption made earlier in this section on absence of magnetic torque within our actuation technique. Instead of driving a coil (i) with steady current (I_i) corresponding to the solution of (5), we use the following oscillatory currents instead

$$I^o_i(t) = I_i \sin(2\pi\omega_i t + \phi_i). \tag{6}$$

Both the frequency $(\omega_i \in \mathbb{R}_+)$ and the phase $(\phi_i \in \mathbb{S})$ of the currents are synchronized for each coil.

Under such conditions, the values of $I^o_i(t)$ oscillate continuously in a synchronous manner, crossing the zero point simultaneously. When the crossing happens, the microbead experiences short-lasting magnetic torque. This effect is used to perturb the microbead, generating rolling motion, which overcomes the static friction. As the currents increase, the bead re-magnetises and follows in direction of the magnetic force $(\mathbf{F}^o_a(t) = \mathbf{F}_a \sin(2\pi\omega_i t + \phi_i))$ acting on the bead [26].

VI. Results and Discussion

The results of the proof-of-concept study are presented in Figure 8, as well as **in supporting video material accompanying this publication.** The control algorithm presented in the previous section is implemented in the experimental setup presented in Figure 6. The control cycle is timed at 45 [Hz], limited by the frame rate of the optical camera.

Our control algorithm is used to drive the currents inside the miniaturized electromagnets of the MILiMAC. The resulting magnetic force acting on the bead affects the direction and the magnitude of its rolling motion. As a result, the microbead successfully accomplishes three trajectories defined by the user. These trajectories comprise of a number of target points, arbitrarily selected through the user-guided interface.

Across three representative trajectories presented in this paper the largest mean error is 0.81 [mm] for Trajectory 1. Given these values are comparable to the size of the microbead itself (0.6 [mm]), and much smaller than the total size of the workspace (triangle side 16 [mm]), we can consider our steering successful. The steady-state behaviour of our system is generally better than the transient one due to lack of high-frequency oscillations, visibly introduced by the rolling motion. Thus, we additionally quantify the error only during these intervals, when the reference location position remains constant. During these intervals, the largest mean error across all trajectories is reported to be 0.41 [mm].

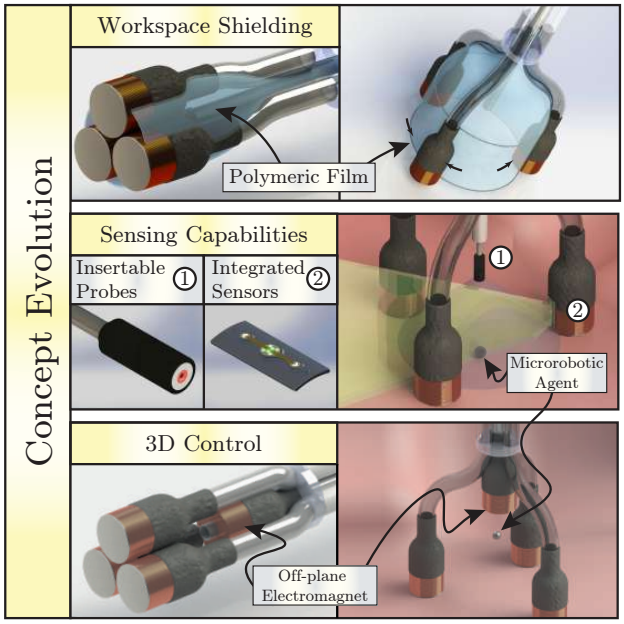

Fig. 9. We envision the concept of a flexible catheter with miniaturized electromagnet to evolve gradually towards clinically-relevant designs. We propose three such improvements, which illustrate the potential of current design. First, the structure of the catheter can be used to support sheets of polymeric film to shield the microrobotic workspace from external disturbance, such as fluid flow. Secondly, catheter can be used as a platform for on-site sensing of the agents, using miniaturized optical and ultrasound devices. Finally, three-dimensional actuation of a micro-agent can be enabled, by integrating additional off-plane electromagnets into the body of the device.

When using electromagnets inside human body, care has to be taken to ensure that the thermal energy dissipated by these devices does not damage the surrounding tissues. We quantify that energy by calculating the root mean square power (RMS) dissipated for each coil during the time intervals, when it is active. We do that using the data describing the instantaneous coil currents along each trajectory, as prescribed by (6). The maximum RMS dissipated power is 0.96 [W], which is almost two orders of magnitude less than the power used in destructive procedures, such as cardiac ablation (50 [W]). [27] This allows us for positive evaluation of the thermal safety of MILiMAC.

The results of the proof-of-concept study indicate, that miniaturized electromagnets constitute a promising alternative to macroscale magnetic actuation system. Located on instruments for minimally-invasive surgery, miniaturized electromagnets are capable of providing effective local magnetic actuation in deeply seated target areas. Furthermore, the study allowed us to identify several key limitations of our current concept, which have to be tackled as the next steps on the road towards clinical applications.

During the deployment phase, we have successfully managed to use the magnetic repulsion between the coils to deploy MILiMAC around the target workspace. Nevertheless, the approximate average deflection of a tether from the initial position, as measured from from the camera images, was only 14 [mm] for the current of 2 [A]. Therefore, imprecise manual manipulation at the base of the insertion channel was still required to position MILiMAC around the reservoir. A possible way of addressing that problem involves the use of externally-generated strong magnetic field around the target workspace to exert magnetic torques on the tethers. These torques would allow for large and precisely controlled deflections enabling positioning of MILiMAC tethers using techniques developed for steering magnetic catheters. [19], [20]

Considering the results of the proof-of-concept steering experiment, the transient behaviour of the microbead still needs to be significantly improved, to reduce the steering errors to values comparable with macroscale magnetic actuation systems (0.1-0.2 [mm]). As our control approach involved a simple PI action with heuristically determined gains and a significantly simplified model of the magnetization of the bead, improvements could involve a more advanced controller, based on a realistic, quadratic model of the actuation [15]. The main factor degrading the performance of the system is significant static friction between the microbeads and the surface, which necessitates using imprecise rolling motion. As friction is inherently determined by the nature of contact between the agent and the environment, we expect the significance thereof to be reduced by using agents exhibiting low friction in body environment. Ultimately, the problem vanishes for proceduress involving agents completely suspended in fluid environment.

Another important limitation involves phenomenon most readily visible in Trajectories 1 and 3, where the bead deviates extensively from the path at times. We attribute these deviations to the unmodelled influenece from the unpowered coil, magnetized nevertheless due to cross-talk. Cross-talk is usually not observed in macroscale magnetic actuation systems employing standard configurations, such as these described in [14]. However, its significance increases at smaller scales, thus is likely to occur in our miniaturized electromagnets, especially if they are kept in parallel. This particular behaviour can be reduced by including hall-effect sensors and controlling miniaturized electromagnets in a closed-loop manner [19].

A separate challenge involves a possibility of electromagnet displacement within the target site, either due to biological motion, or mutual attraction of the magnets (conversely to repulsion used to deploy the system). In case of our proof-of-concept experiment, we rely on friction as well as on the presence of triangular reservoir within the workspace. In clinical setting this problem can be solved by either real-time tracking of electromagnet positions, or by integrating them on surgical instruments, such as needles, which offer improved stability with respect to the environment. For superficial procedures, miniaturized electromagnets could be potentially attached to the skin of the patient.

It is important at this point to stress that MILiMAC is a prototype device. We envision several ways, in which the concept of a surgical instrument with miniaturized electromagnets can evolve (Figure 9). Since our strategy assumes creation of a well-defined workspace, sheets of elastic polymeric film can be fitted between the tethers of MILiMAC to seal the workspace from physiological disturbance. Furthermore, millimetre-sized ultrasound transducers or optical devices could be integrated into the body of MILiMAC, or inserted through its central channel for local tracking of micro-agents and their environment. [28], [29]. Finally, additional off-plane electromagnets can be integrated into the body of MILiMAC to enable three-dimensional actuation of microrobots. Such actuation is desirable, as it not only

ultimately allows for 3D control of microrobots, but can also be exploited for planar manipulation in situations, where the effects of gravity on the motion of the microrobot cannot be neglected.

VII. Conclusions and Future Work

In this paper we reconsider the classical infrastructure used for control of medical micro-agents. Informed by results indicating that miniaturized electromagnets offer larger actuation forces than conventional macroscale system, we present MILiMAC. MILiMAC is equipped with three miniaturized electromagnets located on distal end of a multilumen catheter, and can be navigated into a deeply seated microsurgery site in a minimally-invasive fashion. Upon deployment, MILiMAC creates a target workspace, in which magnetic micro-agents can be controlled using magnetic field generated by miniaturized electromagnets. We test MILiMAC in a proof-of-concept experiment, demonstrating closed-loop position control of a ferrmagnetic microbead using feedback from optical camera.

Since the proof-of-concept study presented in this paper introduces a novel approach, we believe a large body of future work will follow, bringing MILiMAC ever closer towards clinical use. Initially, we plan to enhance our catheter, integrating extensions shown in Figure 9. We aim at showing successful 2D control of micro-agents in a shielded workspace under the guidance of clinically-relevant imaging modality, while exploring control approaches based on accurate interaction models to account for the variable dipole moment of the ferromagnetic bead and to better counter environmental disturbances, such as stiction. Furthermore, we plan to develop a flexible catheter capable of providing three-dimensional, 5DoF actuation of micro-agents, en par with state-of-the-art microrobotic systems. Finally, we plan make use of the findings presented to inform advanced surgical instruments for well-defined procedures executed using micro-agents.

References

[1] B. J. Nelson, I. K. Kaliakatsos, and J. J. Abbott, "Microrobots for minimally invasive medicine," *Annual Review of Biomedical Engineering*, vol. 12, pp. 55–85, 2010.

[2] M. Sitti, H. Ceylan, W. Hu, J. Giltinan, M. Turan, S. Yim, and E. Diller, "Biomedical applications of untethered mobile milli/microrobots," *Proceedings of the IEEE*, vol. 103, no. 2, pp. 205–224, 2015.

[3] S. Scheggi, K. K. T. Chandrasekar, C. Yoon, B. Sawaryn, G. van de Steeg, D. H. Gracias, and S. Misra, "Magnetic motion control and planning of untethered soft grippers using ultrasound image feedback," in *Proceedings of the 2017 IEEE International Conference on Robotics and Automation (ICRA)*, 2017, pp. 6156–6161.

[4] S. Jeon, S. Kim, S. Ha, S. Lee, E. Kim, S. Y. Kim, S. H. Park, J. H. Jeon, S. W. Kim, C. Moon, B. J. Nelson, J.-y. Kim, S.-W. Yu, and H. Choi, "Magnetically actuated microrobots as a platform for stem cell transplantation," *Science Robotics*, vol. 4, no. 30, 2019.

[5] J. Lapointe and S. Martel, "Thermoresponsive hydrogel with embedded magnetic nanoparticles for the implementation of shrinkable medical microrobots and for targeting and drug delivery applications," in *Proceedings of the 2009 Annual International Conference of the IEEE Engineering in Medicine and Biology Society (EBMS)*, 2009, pp. 4246–4249.

[6] B. R. Donald, C. G. Levey, I. Paprotny, and D. Rus, "Planning and control for microassembly of structures composed of stress-engineered MEMS microrobots," *The International Journal of Robotics Research*, vol. 32, no. 2, pp. 218–246, 2013.

[7] V. Magdanz, M. Guix, and O. G. Schmidt, "Tubular micromotors: from microjets to spermbots," *Robotics and Biomimetics*, vol. 1, no. 1, pp. 1–10, 2014.

[8] X. Yan, Q. Zhou, M. Vincent, Y. Deng, J. Yu, J. Xu, T. Xu, T. Tang, L. Bian, Y.-X. J. Wang *et al.*, "Multifunctional biohybrid magnetite microrobots for imaging-guided therapy," *Science Robotics*, vol. 2, no. 12, 2017.

[9] P. Fischer, B. J. Nelson, and G.-Z. Yang, "New materials for next-generation robots," *Science Robotics*, vol. 3, no. 18, 2018.

[10] J. J. Abbott, E. Diller, and A. J. Petruska, "Magnetic methods in robotics," *Annual Review of Control, Robotics, and Autonomous Systems*, vol. 3, 2019.

[11] S. Pané, J. Puigmartí-Luis, C. Bergeles, X.-Z. Chen, E. Pellicer, J. Sort, V. Počepcová, A. Ferreira, and B. J. Nelson, "Imaging technologies for biomedical micro-and nanoswimmers," *Advanced Materials Technologies*, vol. 4, no. 4, p. 1800575, 2019.

[12] T. Xu, J. Yu, X. Yan, H. Choi, and L. Zhang, "Magnetic actuation based motion control for microrobots: An overview," *Micromachines*, vol. 6, no. 9, pp. 1346–1364, 2015.

[13] M. P. Kummer, J. J. Abbott, B. E. Kratochvil, R. Borer, A. Sengul, and B. J. Nelson, "OctoMag: An electromagnetic system for 5-DOF wireless micromanipulation," *IEEE Transactions on Robotics*, vol. 26, no. 6, pp. 1006–1017, 2010.

[14] A. Pourkand and J. J. Abbott, "A critical analysis of eight-electromagnet manipulation systems: The role of electromagnet configuration on strength, isotropy, and access," *IEEE Robotics and Automation Letters*, vol. 3, no. 4, pp. 2957–2962, 2018.

[15] F. Ongaro, S. Pane, S. Scheggi, and S. Misra, "Design of an electromagnetic setup for independent three-dimensional control of pairs of identical and nonidentical microrobots," *IEEE Transactions on Robotics*, vol. 35, no. 1, pp. 174–183, 2018.

[16] P. R. Slawinski, A. Z. Taddese, K. B. Musto, K. L. Obstein, and P. Valdastri, "Autonomous retroflexion of a magnetic flexible endoscope," *IEEE Robotics and Automation Letters*, vol. 2, no. 3, pp. 1352–1359, 2017.

[17] S. E. Wright, A. W. Mahoney, K. M. Popek, and J. J. Abbott, "The spherical-actuator-magnet manipulator: A permanent-magnet robotic end-effector," *IEEE Transactions on Robotics*, vol. 33, no. 5, pp. 1013–1024, 2017.

[18] L. Yang, X. Du, E. Yu, D. Jin, and L. Zhang, "DeltaMag: An electromagnetic manipulation system with parallel mobile coils," in *Proceedings of the 2019 International Conference on Robotics and Automation (ICRA)*, 2019, pp. 9814–9820.

[19] J. Sikorski, C. M. Heunis, F. Franco, and S. Misra, "The ARMM system: An optimized mobile electromagnetic coil for non-linear actuation of flexible surgical instruments," *IEEE Transactions on Magnetics*, vol. 55, no. 9, pp. 1–9, 2019.

[20] J. Edelmann, A. J. Petruska, and B. J. Nelson, "Magnetic control of continuum devices," *International Journal of Robotics Research*, vol. 36, no. 1, pp. 68–85, 2017.

[21] G. J. Vrooijink, A. Denasi, J. G. Grandjean, and S. Misra, "Model predictive control of a robotically actuated delivery sheath for beating heart compensation," *International Journal of Robotics Research*, vol. 36, no. 2, pp. 193–209, 2017.

[22] A. Servant, F. Qiu, M. Mazza, K. Kostarelos, and B. J. Nelson, "Controlled in vivo swimming of a swarm of bacteria-like microrobotic flagella," *Advanced Materials*, vol. 27, no. 19, pp. 2981–2988, 2015.

[23] C. M. Heunis, J. Sikorski, and S. Misra, "Flexible instruments for endovascular interventions: improved magnetic steering, actuation, and image-guided surgical instruments," *IEEE Robotics and Automation Magazine*, vol. 25, no. 3, pp. 71–82, 2018.

[24] N. Jaffrezic-Renault, C. Martelet, Y. Chevolot, and J.-P. Cloarec, "Biosensors and bio-bar code assays based on biofunctionalized magnetic microbeads," *Sensors*, vol. 7, no. 4, pp. 589–614, 2007.

[25] F. Ongaro, D. Niehoff, S. Mohanty, and S. Misra, "A contactless and biocompatible approach for 3d active microrobotic targeted drug delivery," *Micromachines*, vol. 10, no. 8, p. 504, 2019.

[26] M. T. Hou, H.-M. Shen, G.-L. Jiang, C.-N. Lu, I.-J. Hsu, and J. A. Yeh, "A rolling locomotion method for untethered magnetic microrobots," *Applied Physics Letters*, vol. 96, no. 2, p. 024102, 2010.

[27] W. Saliba, V. Y. Reddy, O. Wazni, J. E. Cummings, J. D. Burkhardt, M. Haissaguerre, J. Kautzner, P. Peichl, P. Neuzil, V. Schibgilla *et al.*, "Atrial fibrillation ablation using a robotic catheter remote control system: initial human experience and long-term follow-up results," *Journal of the American College of Cardiology*, vol. 51, no. 25, pp. 2407–2411, 2008.

[28] A. Katouzian, E. D. Angelini, S. G. Carlier, J. S. Suri, N. Navab, and A. F. Laine, "A state-of-the-art review on segmentation algorithms in intravascular ultrasound (IVUS) images," *IEEE Transactions on Information Technology in Biomedicine*, vol. 16, no. 5, pp. 823–834, 2012.

[29] T. Yamakawa, T. Inoue, Y. He, M. Fujii, M. Suzuki, and M. Niwayama, "Development of an implantable flexible probe for simultaneous near-infrared spectroscopy and electrocorticography," *IEEE Transactions on Biomedical Engineering*, vol. 61, no. 2, pp. 388–395, 2014.